

Review Article

Seismic sequence near Zakynthos Island, Greece, April 2006: Identification of the activated fault plane

A. Serpetsidaki^{a,*}, E. Sokos^a, G.-A. Tselentis^a, J. Zahradnik^b^a University of Patras, Seismological Laboratory, Patras, Greece^b Charles University, Faculty of Mathematics and Physics, Prague, Czech Republic

ARTICLE INFO

Article history:

Received 13 April 2009

Received in revised form 24 September 2009

Accepted 24 September 2009

Available online 3 October 2009

Keywords:

Waveform inversion

Focal mechanisms

Centroid moment tensor

Fault plane

Iterative deconvolution

Zakynthos Island

ABSTRACT

The April 2006 earthquake sequence near Zakynthos (Western Greece) is analysed to identify the fault plane(-s). The sequence (33 events) was relocated to assess physical insight into the hypocenter uncertainty. Moment tensor solution of three major events was performed, simultaneously with the determination of the centroid position. Joint analysis of the hypocenter position, centroid position and nodal planes indicated sub-horizontal fault planes. Moment tensor solutions of 15 smaller events were performed under assumption that the source positions are those of the hypocenters (without seeking centroids). Their focal mechanisms are highly similar and agree with the analysis of the three major events. The preferable seismotectonic interpretation is that the whole sequence activated a single sub-horizontal fault zone at a depth of about 13 km, corresponding to the interplate subduction boundary. Considering that the Ionian Sea is a high-seismicity area, the identification of the seismic fault is significant for the seismic hazard investigation of the region.

© 2009 Elsevier B.V. All rights reserved.

Contents

1. Introduction	23
2. Location	24
3. Moment tensors	25
4. Discussion and conclusion	28
Acknowledgements	31
References	31

1. Introduction

Starting on April 3, 2006, a moderate size sequence occurred in the Ionian Sea, South of the Zakynthos Island. The sequence lasted for a month; through which the permanent seismological networks of Greece recorded tenths of weak events. During the first 15 days, the seismicity was denser, while in this period the largest events took place. The Magnitude of the 9 strongest events of the sequence varied between 4.5R and 5.5R; the majority of the events occurred in depth shallower than 20 km.

Zakynthos Island is located in the Ionian Sea, at the western part of the Hellenic Arc. The Eastern Mediterranean lithosphere is being subducted there beneath the Aegean lithosphere along the Hellenic Arc and this sets the Ionian Sea as a seismotectonically complex area of high seismicity. The regional seismicity of Western Greece, including the Ionian Islands has been extensively studied recently (Van Hinsbergen et al., 2006; Roumelioti et al., 2007; Kiratzi et al., 2008; Chouliaras, 2009). Nevertheless, strong earthquakes and seismic sequences provided the chance for local seismicity studies (Sachpazi et al., 2000; Benetatos et al., 2005; Zahradnik et al., 2005; Tselentis et al., 2006a,b). Their results indicate that in the western part of the arc, in the Ionian Sea the thickness of the shallow seismogenic layer covers the upper 20 km of the crust.

The main structures, which compose the seismotectonic regime of the area, are the Hellenic subduction, the Cephalonia transform fault and the Ionian thrust (Fig. 1). During investigations carried out by Hirn

* Corresponding author.

E-mail addresses: annaserp@upatras.gr (A. Serpetsidaki), jiri.zahradnik@mff.cuni.cz (J. Zahradnik).

et al. (1996), Sachpazi et al. (2000), Clement et al. (2000) and Laigle et al. (2004), reflection and refraction data confirmed the existence of a reflector imaged at 13 km depth, dipping slightly to the East and becoming steeper landward. The reflector has been interpreted as being the subduction interplate boundary; it has been suggested to be the interface along which the western Hellenides override Africa in the presently active subduction (Hirn et al., 1996). The Cephalonia transform fault is a major strike-slip fault that links the subduction boundary to the continental collision between the Apulian microplate and the Hellenic foreland (Sachpazi et al., 2000; Zahradnik et al., 2005). Major earthquakes in the area corresponding to thrust faults were also modeled and designated to the Cephalonia fault or they are clearly associated with the Ionian Subduction (Clement et al., 2000; Papadimitriou, 1993; Anderson and Jackson, 1987; Kiratzi and Louvari 2003) (Fig. 1).

Therefore, delineating the earthquake-activated fault planes for a complex area like this is challenging. The aim of this paper is to introduce an innovative procedure for the identification of the fault plane. It is based on combination of the hypocentre relocations and moment tensor (MT) solutions, both with an emphasis on the uncertainty estimation. For major events of the sequence the MT solution can include also calculation of the centroid position. Then the fault plane is one of the nodal planes passing through the centroid, that one which contains the hypocenter. For smaller events, for which the centroid and hypocenter are closer to each other, the MT is calculated just for the hypocentre position, and we investigate the relation of such MT solutions with the possible fault plane suggested by the major events.

2. Location

The study of the April 2006 Zakynthos sequence focuses in 33 events, which are presented in Table 1. The selected events of local magnitude ranging from 3.3 to 5.4, occurred in the studied region during the period from April 3 to April 19 of 2006. Location was performed by 30 stations (PSLNET, NOA and ITSAK) shown in Fig. 2. Manual picks of the P and S waves were only used, the number of which is presented in Table 1. In the first stage of the procedure, the hypocenters were located using the HYPO71 code; in the second stage the HYPODD code was implemented to relocate the events.

During the location first stage, several tests carried out in order to use the most appropriate 1D model and decide the parameters that would lead to the most stable results. Three 1D crustal models (Table 2) were employed: M1 is the Jeffreys–Bullen model with its top 3 km modified to have $V_p = 3.5$ km/s. M2 and M3 are taken from Haslinger et al. (1999), and Tselentis et al. (1996), respectively. The criteria for choosing the most suitable crustal model were the standard RMS, ERH, ERZ errors calculated by the HYPO71.

In the beginning the whole 33-events dataset was used; setting the ratio $V_p/V_s = 1.75$ and the trial (“starting”) depth to 10 km, the 3 models were tested. Irrespectively of the model, most of the events were found in a relatively well-defined zone South of the Island of Zakynthos. The errors showed that the preferable model (leading to the smallest error) is model M3. The M3 model corresponding locations are listed in Table 1.

Another reason to prefer the M3 model comes from the stability test in terms of the trial source depth in HYPO71. We varied the trial depth (2, 4, ... km) and observed its effect upon the location depth.

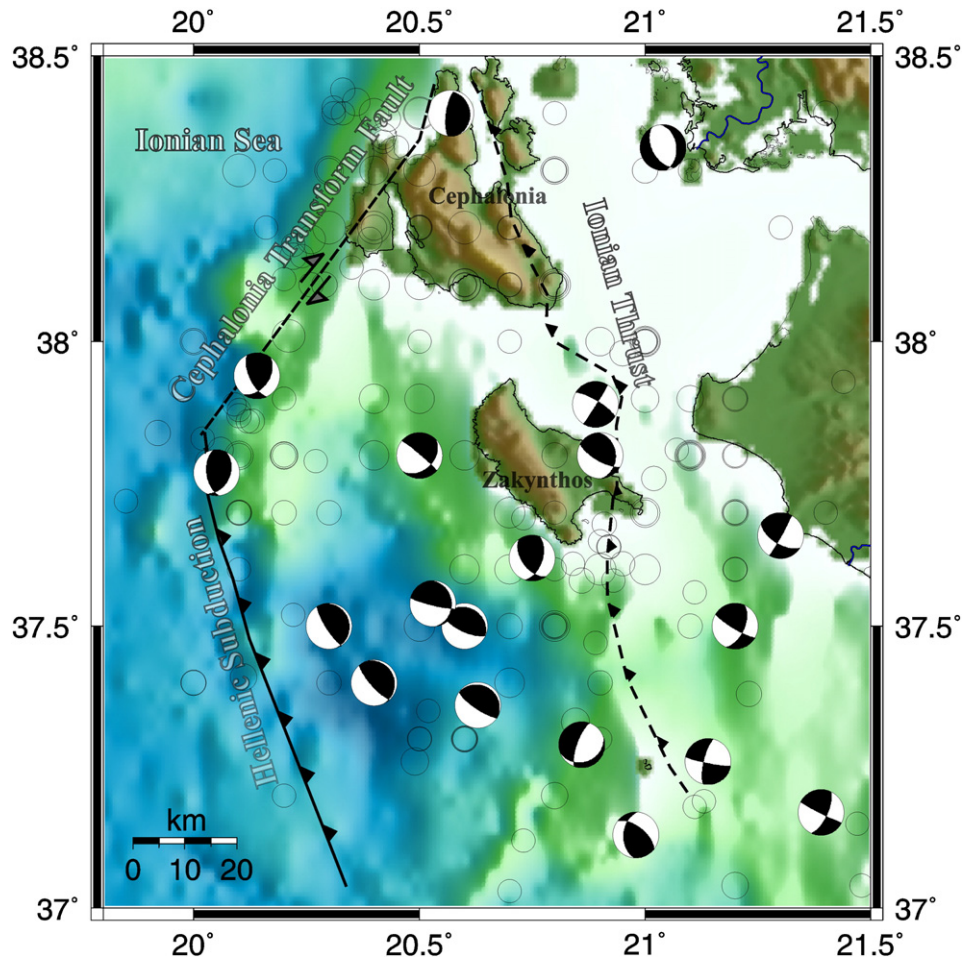


Fig. 1. Seismotectonic map of Central-South Ionian Sea (Underhill, 1988, 1989). Focal mechanism solutions were calculated by Kiratzi and Louvari (2003). Black circles correspond to historical and recent earthquakes with $M > 5$ (catalogue information www.gein.noa.gr, 400BC up 2006, Roumelioti et al., 2007).

Table 1

The 2006 Zakynthos sequence as located in this paper by HYPO71 and HYPODD.

#	Date	Origin	HYPO71			No P&S	RMS	ERH	ERZ	M_L	HYPODD		
			Latitude (degrees)	Longitude (degrees)	Depth (km)						Latitude (degrees)	Longitude (degrees)	Depth (km)
1	2006 04 3	00 49 43	37.58	20.95	13	26	.56	1.9	1.6	4.8	37.58	20.93	15
2	2006 04 4	22 05 03	37.57	20.90	12	32	.85	3.7	3.5	5.2	37.58	20.91	12
3	2006 04 9	07 06 26	37.67	20.99	1	28	.60	1.7	3.0	3.9			
4	2006 04 10	21 10 21	37.69	20.93	12	28	.78	2.5	2.2	4.0	37.67	20.93	12
5	2006 04 10	21 21 24	37.63	20.90	5	31	.81	2.7	3.2	4.2	37.63	20.93	9
6	2006 04 11	00 02 42	37.62	20.90	11	26	.54	2.0	1.8	5.2	37.62	20.90	13
7	2006 04 11	01 02 36	37.60	20.90	12	21	.58	2.4	2.2	4.0	37.60	20.92	11
8	2006 04 11	07 07 37	37.63	20.87	3	23	.71	2.8	4.3	3.8	37.63	20.89	13
9	2006 04 11	17 29 28	37.68	20.90	11	35	.67	2.1	1.9	5.4	37.66	20.90	13
10	2006 04 12	01 20 45	37.52	20.94	3	23	.85	3.6	7.2	3.7	37.55	20.98	13
11	2006 04 12	16 52 01	37.59	20.92	15	36	.71	2.6	2.3	5.4	37.60	20.93	14
12	2006 04 12	16 56 24	37.64	20.85	4	24	1.03	4.1	6.4	4.7	37.63	20.87	10
13	2006 04 12	17 55 24	37.67	20.93	6	27	.89	3.2	3.2	4.0	37.64	20.89	8
14	2006 04 12	21 22 51	37.69	20.69	1	11	.71	4.1	6.4	3.8			
15	2006 04 12	21 27 57	37.68	20.92	11	23	.88	3.2	3.3	4.0	37.67	20.92	15
16	2006 04 12	22 04 49	37.67	20.90	13	21	.78	3.3	3.8	3.7	37.68	20.88	17
17	2006 04 12	23 54 14	37.70	20.89	14	24	.64	2.7	2.7	3.8	37.68	20.87	16
18	2006 04 12	23 57 40	37.61	20.90	9	29	.73	2.5	2.5	4.0	37.61	20.89	13
19	2006 04 13	03 20 29	37.66	20.90	7	21	.67	2.5	3.0	3.7	37.66	20.88	12
20	2006 04 13	23 21 43	37.66	20.90	11	25	.87	3.3	3.2	3.9	37.66	20.88	16
21	2006 04 13	23 25 28	37.72	20.85	28	29	1.27	7.6	4.8	4.1			
22	2006 04 14	01 10 26	37.55	20.98	1	19	.88	3.5	7.5	3.6			
23	2006 04 14	01 40 19	37.53	20.93	0	20	.96	4.2	8.0	3.6			
24	2006 04 14	19 50 01	37.66	21.05	2	12	1.15	7.4	2.2	3.4			
25	2006 04 14	21 21 30	37.60	20.92	3	25	.99	3.2	5.6	3.7			
26	2006 04 15	00 50 06	37.60	21.06	1	21	1.37	4.2	9.5	3.5			
27	2006 04 15	02 18 17	37.79	20.97	7	10	1.09	5.9	8.4	3.3	37.78	20.98	13
28	2006 04 15	21 15 11	37.62	20.94	13	34	.81	3.5	3.5	4.8	37.62	20.97	11
29	2006 04 16	00 43 31	37.61	21.04	1	25	.91	2.5	5.0	3.6			
30	2006 04 16	03 07 32	37.56	20.94	12	14	.97	4.9	5.2	3.5	37.59	20.96	6
31	2006 04 16	06 33 07	37.59	20.88	2	15	.67	3.5	6.9	3.7	37.59	20.85	5
32	2006 04 17	08 54 40	37.68	20.97	10	25	.83	2.2	2.2	4.7	37.61	20.97	10
33	2006 04 19	15 16 26	37.77	20.88	22	23	.57	3.0	2.9	4.7	37.66	20.81	11

M_L is local magnitude of NOA. Three major events are in bold. The velocity model, used in calculations, is the model referred to as M3 in this study.

Model M2 produced the least stable results, due to the large number of layers in that model and low velocities in the topmost layers. The instability is related to head waves from intra-crustal discontinuities. On the contrary, model M3, with its low number of layers and relatively large velocities at its top, is the most stable. Model M1 is an intermediate case. The stability test like this is important for preventing the unstable solutions. However, it cannot be used for optimizing the depth estimate. By, varying the trial depth, not only the resulting hypocenter depth varies, but also the resulting epicenter is shifted. The horizontal and vertical positions move in such a way that the RMS misfit stays constant; hence none of the depths can be preferred.

The next tests were performed for the three major events of the sequence (those highlighted in Table 1). The values of the ratio V_p/V_s were varied (1.74, 1.75... 1.78); the results showed that the M3 model was still the most appropriate. Additionally the M3 model with the V_p/V_s ratio value of 1.76 was the optimum combination. To improve the depth estimate of the three major events, the following method was used. For each event, its HYPO71 epicenter was kept fixed, and the depth was found by grid-search minimization of the travel-time residual. This useful trick aims at overcoming the unfavorable fact that the time residuals are affected by the depth variation much less than by the epicenter variation. If retrieving both the depth and the horizontal position, the depth resolution is low. That is why we decouple the depth by fixing the epicenter. Moreover, the grid search is free from limitations of the linearization used in HYPO71. The results showed that the depth optimized in this way, for the three major events, is between 12 and 14 km. The corresponding hypocenters are listed in Table 3.

Finally, based on the stability of the M3 model, the whole sequence was relocated using HYPODD, (Table 1). Catalog P- and S-wave data (5055 and 1169, respectively) were used in the procedure derived from

stations within 500 km from the centre of the initial epicentral area. 32 initial sources and 29 stations were combined in the procedure, and parameters were set, following Waldhauser's (2001) suggestions for datasets containing small number of events. The maximum number of neighbour events was set to the number of the initial sources (33). The double-difference residuals for the pairs of earthquakes at each station were minimized by weighted least squares using the method of singular value decomposition. The 1D velocity model to calculate the theoretical travel-times was the M3 (Table 2), the one that was established by the first stages tests. Initial locations (sources) were primarily taken from the derived HYPO71PC catalog at reported locations and next at a common location at the 'center of gravity' of the cluster. The results from both methods agree with each other within 100 m.

The HYPODD final results include the 73% of the initial dataset (24 relocated events). The HYPODD final results show a mean RMS of 0.01 s and a mean x, y, z, t formal inaccuracy of 47 m, 40 m, 57 m, and 17 ms, respectively. The HYPODD relocation epicenters form a single cluster and show a spatial pattern, which is more compact, compared to HYPO71 solution. The events located by HYPO71 and the relocated by HYPODD are presented in Fig. 3, with crosses and circles, respectively. Most of the events are located in the sea area SSE of the Zakynthos Island and the greater percentage of the hypocenters are situated in the depths of about 15 km, while the three larger events ($M \sim 5.5$) occur in the depth of 13 km.

3. Moment tensors

Moment tensors of 24 events of the sequence were calculated by waveform inversion of three-component broadband records of PSLNET. The network, which belongs to the Seismological Laboratory of the University of Patras, is a new satellite telemetry network, starting

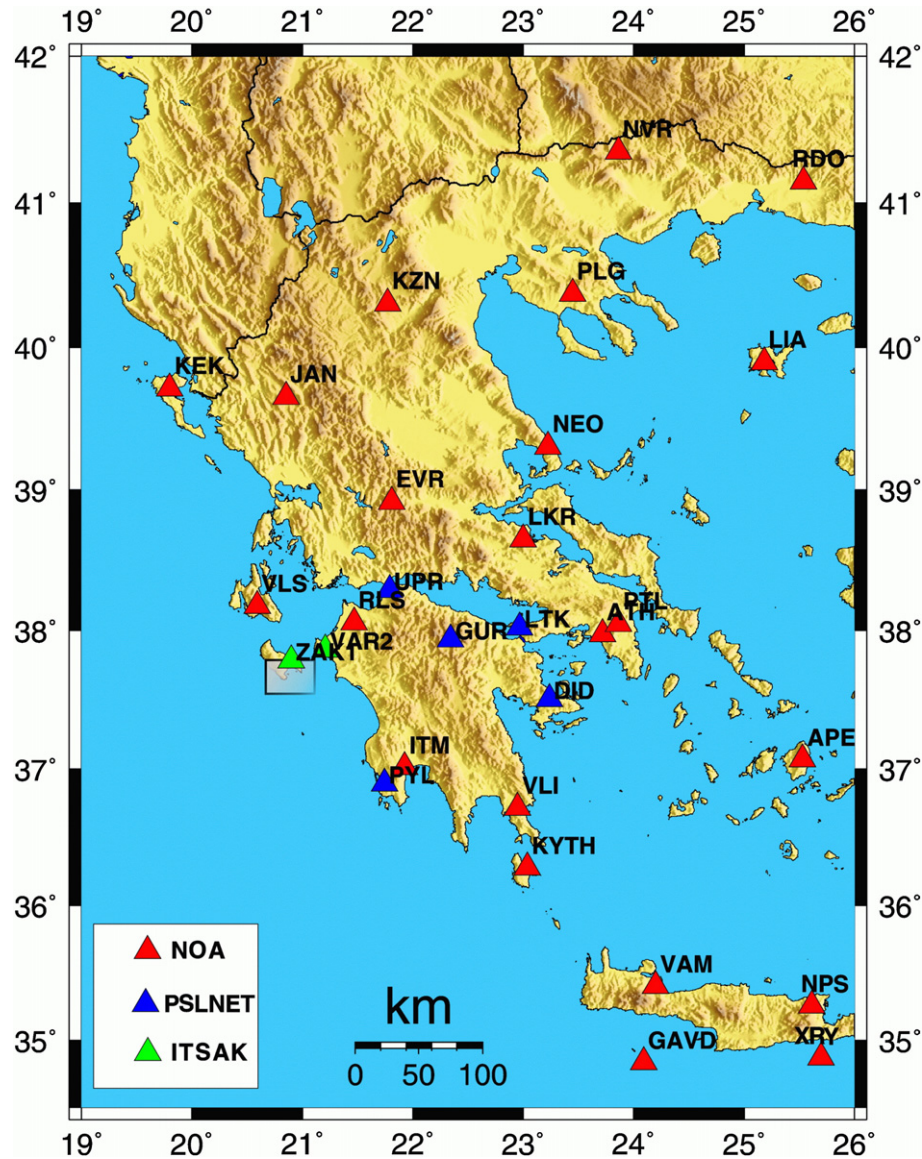


Fig. 2. Stations used for the location. Most of them are broadband stations, except a few strong motions stations (ZAK1 and VAR2) and analogue stations (PTL, KYTH, XRY, and GAVD). The stations belong to three networks as shown in the legend. The studied area around Zakyntos Island is highlighted by a small rectangle.

operation in 2006 shortly before the sequence. The stations are equipped with Trillium 40 sensors, Trident digitisers and use Libra VSAT (Nanometrics). More details and present status of the network can be found at <http://seismo.geology.upatras.gr>.

Table 2
Three crustal models with homogeneous layers used for the location.

M1		M2		M3	
Vp (km/s)	Depth (km)	Vp (km/s)	Depth (km)	Vp (km/s)	Depth (km)
3.50	0	3.50	0	5.70	0
5.57	3	5.47	0.5	6.00	5
6.50	18	5.50	2	6.40	18
8.10	36	6.00	5	7.90	39
		6.20	10		
		6.48	15		
		6.70	20		
		6.75	30		
		8.00	40		

The $V_p/V_s = 1.76$ was adopted for all the models.

The MT inversion is performed by the so-called iterative deconvolution of Kikuchi and Kanamori (1991), modified for regional distances and newly encoded by Zahradnik et al. (2005). Complete waveforms are used, without separation of individual phases; full-wave Green functions are calculated by the discrete wavenumber method in a 1D velocity model. Easy processing of many events is possible due to a user-friendly Fortran–Matlab program package ISOLA (Sokos and Zahradnik, 2007). The code may retrieve a possibly multiple point-source model (Zahradnik et al., 2005, 2007; Adamova et al., 2007). The present paper focuses on the most robust case of the single-source and deviatoric inversion (no volume change). Following a common deviatoric tensor decomposition approach, the double-couple (DC) part and the compensated linear vector dipole (CLVD) part – as the non-double-couple (non-DC) component – were determined. However, the usefulness of the non-DC component as a physical parameter of tectonic earthquakes is highly limited (Zahradnik et al., 2008) due to the available crustal model, the stations coverage gap etc. Zahradnik et al. (2008) studied the three major events non-DC component, using a different crustal model and an extended double-source representation. The results are expressed in terms of the double-couple component of the deviatoric solution, represented by the scalar moment, strike, dip and rake.

Table 3
Special treatment of the three major events; their hypocenter and centroid positions.

Event #	Hypocentre LAT N (degrees)	Hypocentre LON E (degrees)	Hypocentre depth (km)	Centroid LAT N (degrees)	Centroid LON E (degrees)	Centroid depth (km)
6	37.62	20.90	12	37.70	20.77	7
9	37.68	20.90	12	37.70	20.79	6
11	37.59	20.92	14	37.61	20.86	11

The MT calculation is performed in crustal model M3 (Table 2) and the frequency range is 0.020–0.10 Hz. Those are the lowest available frequencies with a good signal/noise ratio. The low frequencies are preferred because in this case the modeling is less dependent on the (inherently) incomplete knowledge of the crustal structure. Together with the relatively small epicentral distances, <200 km, the results are practically independent of the choice of the available crustal model.

Most inversions (except the three major events) were made for the source position assumed to be identical with the HYPO71 hypocenter. The assumption is based on the fact that for events $M < 4$ the size of ruptured part of the fault plane is comparable to the uncertainty of the hypocenter and centroid position, so there is no reason to seek both. Small adjustments of the depth and/or horizontal position were made in few cases to improve the waveform fit. Fig. 4 shows the waveforms fit for a moment tensor solution; red waveform is the synthetic, black is the observed while, the waveforms in gray depict poor fit consequently they are excluded from the calculations in order to determine a fine solution.

The three major events, $M \sim 5.5$ were also investigated for the mutual position of the hypocenter and centroid, H and C. The centroid was determined by repeated calculations of the MT in a volume grid of trial source positions not far from the hypocenter, aiming at optimizing the fit between the observed and synthetic waveforms. The so-called hierarchic grid search was applied (Zahradnik et al., 2008), using a progressively finer grid while approaching towards the likely centroid position. The optimum source positions (C) were identified at the locations shown in Table 3. Due to the low-frequency nature of the MT waveform inversion, the centroid position cannot be resolved better than with the inaccuracy of a few kilometers (Zahradnik et al., 2008). Nevertheless, it already

approaches the limit enabling the study of the mutual position of H and C, since according to empirical relations for $M \sim 5.5$ earthquakes the fault size is of the order of 6×6 km (Somerville et al., 1999).

All MT solutions are displayed in Table 4 and Fig. 5a; Fig. 5b shows the distribution of the MT solutions across the line AA'. Notable feature of this result is the striking similarity among the mechanisms, throughout the whole activated volume.

Joint knowledge of C, the MT solution (nodal planes) and hypocenter position H is a key to identify the fault plane. Indeed, the nodal planes pass through C, and the fault plane is that one comprising also H. Although the idea is simple, its successful application needs a great caution in the determination of H and C, so it is hardly applicable at a routine processing level. As an example of a problematic case, Fig. 6a compares mutual position of the hypocenter with the centroid and the two nodal planes passing through the centroid for event E6. The data come from two sources, the quick MT determination of MEDNET and the location of EMSC. The figure demonstrates that the hypocenter is far from nodal planes, not enabling identification of any nodal plane as the fault plane. It means that the data are inconsistent, most likely due to errors in both the hypocenter and centroid positions. The other two major events have almost the same behavior. On the contrary, as demonstrated in Fig. 6b,c, and d, using the same procedure with the location and MT data of this paper (Tables 1, 3 and 4), the hypocenters of all three major events clearly prefer the sub-horizontal nodal plane, thus indicating that nodal plane to be the fault plane.

Seeking an additional evidence to prove the leading role of a sub-horizontal rupture plane(-s) during the sequence we find the following: (i) The three major events have similar depth, 12 to 14 km, or 13 km

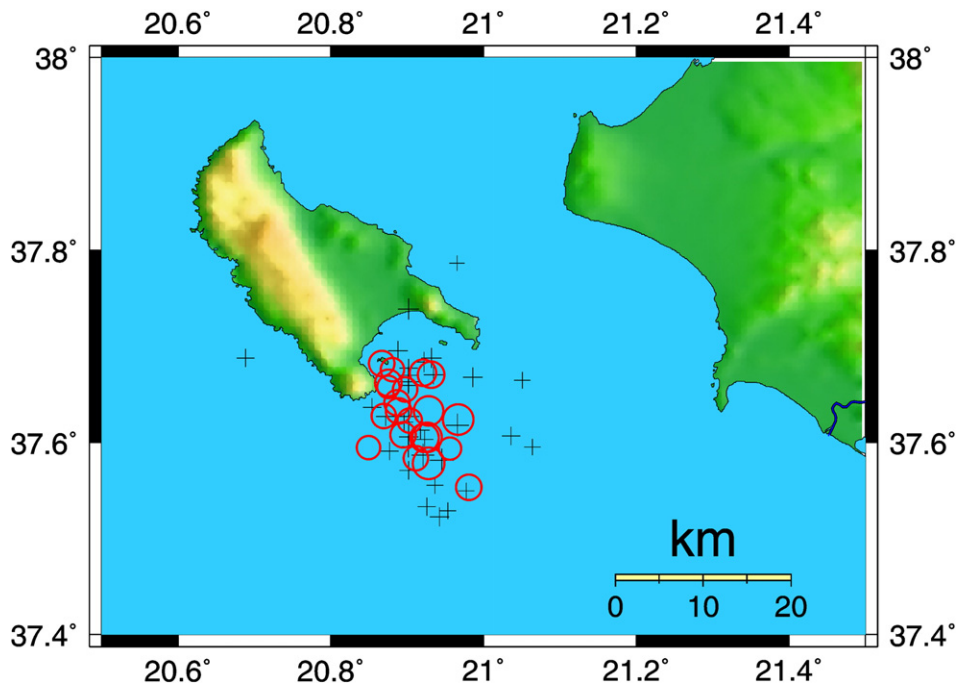


Fig. 3. The studied sequence relocated by the HYPODD method (circles). For comparison, the HYPO71 location is also shown (crosses).

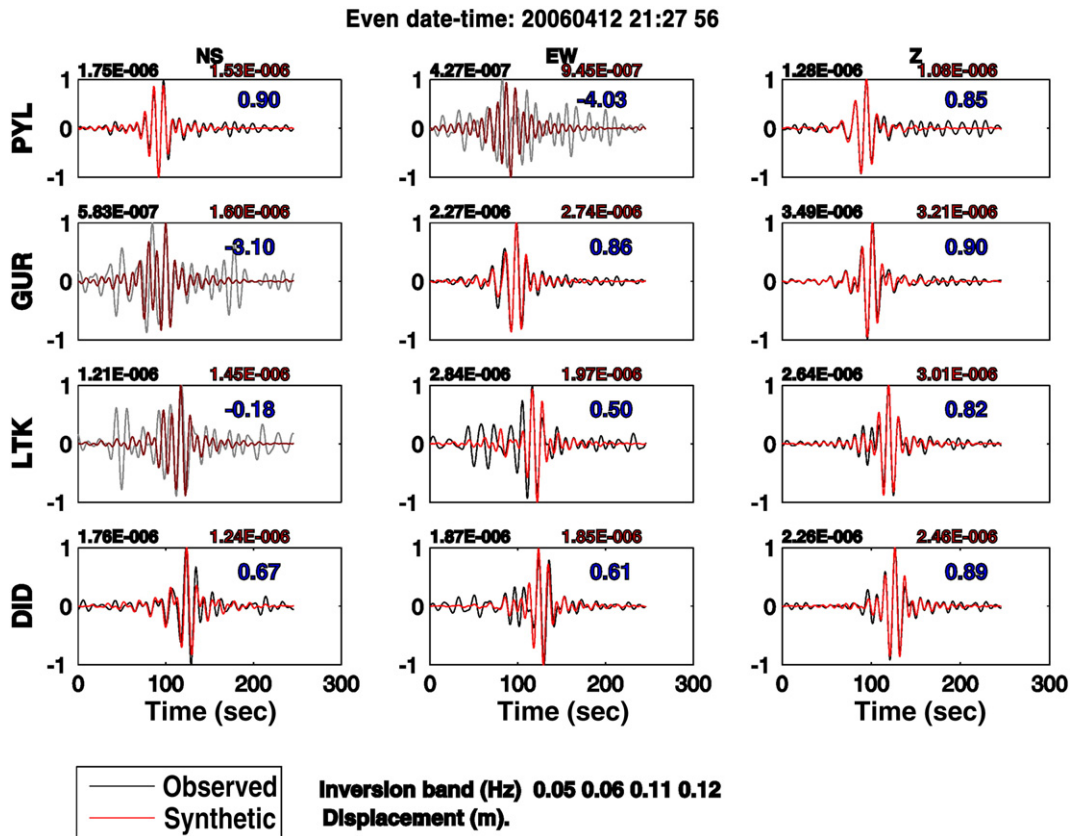


Fig. 4. The waveforms fit for a moment tensor solution; red waveform is the synthetic, black is the observed. The waveforms in gray depict poor fit and they are excluded from the calculations.

(Table 1, the HYPODD result). (ii) Events #6 and #11 are very similar to each other in both fault planes, but event #9 shares with them only one nodal plane – again the sub-horizontal one. (iii) Almost all focal mechanisms demonstrate the presence of one low-dip horizontal nodal

plane (Fig. 5a and b). (iv) The distribution of the hypocenters favors a sub-horizontal plane rather than a sub-vertical.

However, the similarity of the focal mechanisms might suggest also a quite different interpretation, represented by the *other set* of the steeply dipping (sub-vertical) nodal planes. If the sub-vertical nodal planes were the fault planes and the position of the foci was those of the HYPODD location, the fault zone was very thick (its thickness being given by the horizontal extent of the epicenters in Fig. 3, i.e. of about 10 km), unless we accept large horizontal errors in the location. Because accepting larger depth errors is easier, we consider the above interpretation of the sub-horizontal plane to be more likely. The distribution of the hypocenters shows preference to a sub-horizontal plane (Fig. 5b), which is figured by the majority of the events as well as the larger events. Moreover, the sub-vertical nodal plane suggests the existence of a back-thrust structure, which is not supported by any tectonic data of the area.

4. Discussion and conclusion

The Ionian Islands, among them Zakynthos, belong to the most seismic active areas of Mediterranean. The seismotectonic regime is controlled by the relative motions of the Aegean plate, the African plate and the Apulian platform (McKenzie, 1972). The dominant structure in the study area is the Western Hellenic Subduction, where the Aegean plate overrides the Africa plate. The eastern part of the study area includes the Ionian Thrust, where the Ionian zone overthrusts the (Pre-) Apulian Zone (Mercier et al., 1972, 1976; Sorel et al., 1976; Cushing, 1985; Underhill, 1988, 1989; Meco and Aliaj, 2000). Nearly all events that have occurred south of Zakynthos Island have dominantly pure dip-slip thrust mechanisms (Kiritzi and Langston, 1991). In the Southern part between the islands of Zakynthos and Strofadhes the focal mechanisms calculated by Kiritzi and Louvari (2003), show compressional tectonics with a strike-slip component.

Table 4
Focal mechanisms obtained by the MT inversion.

Event #	Moment (Nm)	Strike (deg)	Dip (deg)	Rake (deg)	Number of stations	DC %	Variance Reduction %
1	7.14E+16	151	87	79	2	93	69
3	8.19E+14	162	76	83	2	72	64
4	8.54E+14	154	76	79	3	96	70
5	5.92E+15	156	74	85	3	96	73
6	1.00E+17	157	80	82	3	83	73
7	1.80E+15	147	86	88	3	73	52
8	5.67E+14	259	81	-86	3	60	42
9	1.90E+17	202	83	115	3	21	86
11	1.60E+17	158	80	87	4	58	82
12	3.72E+16	165	75	96	4	37	61
13	8.31E+14	161	76	83	4	59	65
14	5.55E+14	113	46	90	4	96	53
15	1.56E+15	152	72	90	4	76	64
16	7.49E+14	142	88	67	4	15	78
17	4.78E+14	151	55	102	4	29	71
18	6.32E+14	158	81	86	4	50	54
19	1.14E+15	148	90	67	4	40	76
20	1.54E+15	154	65	101	4	97	76
21	2.04E+15	158	71	93	4	91	74
28	2.08E+16	152	78	179	5	59	73
30	5.15E+14	169	73	82	5	61	76
31	4.69E+14	146	73	92	5	60	77
32	1.49E+16	142	87	68	5	55	78
33	4.52E+16	146	73	92	5	60	77

Three major events are in bold.

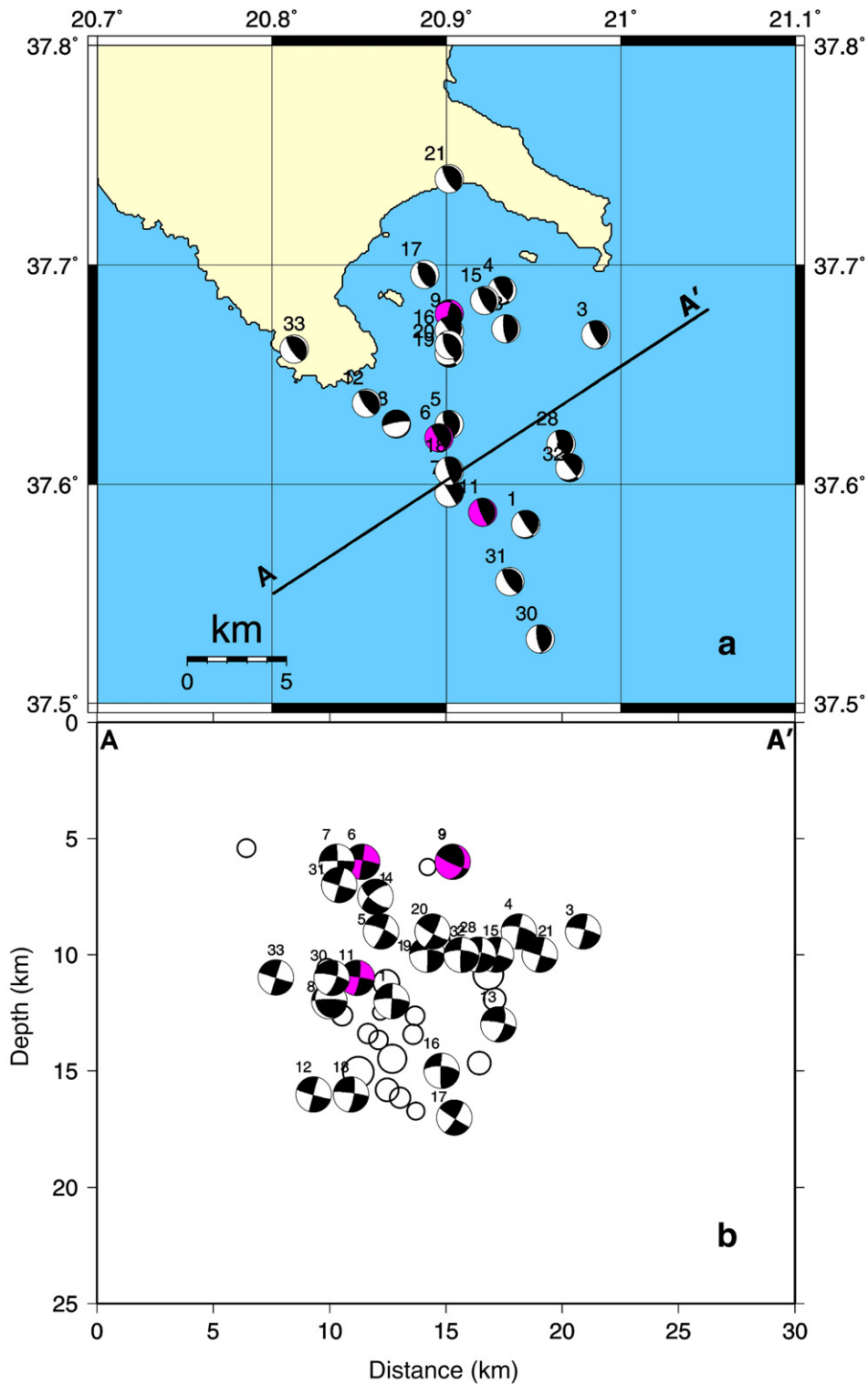


Fig. 5. a) Focal mechanisms obtained from the MT inversion (Table 4). The three major events # 6, 9 and 11, having a special treatment, are plotted in color. b) Projection of the relocated hypocenters and MT solution (accordingly rotated) in depth cross-section AA'.

Reflection surveys in the region image a major reflector at a depth of about 13 km slightly dipping to the east under the western slope of the Ionian islands then dipping steeply under them (Fig. 7) (Hirn et al., 1996; Clement et al., 2000; Laigle et al., 2004). This dipping interface revealed at 13 km depth has been suggested as the interplate boundary of the Western Hellenic subduction (Clement et al., 2000). The Ionian Thrust has been identified (Hirn et al., 1996) either with the western high

(Brooks and Ferentinos, 1984; Stiros et al., 1994) or with the eastern high (Underhill, 1989).

We have located with HYP071, 33 events of the April 2006 earthquake sequence using manual measurements from all Greek permanent networks. We tested three 1D models and selected the one with the best fit (minimum errors); the model is referred to as M3 and was suggested by Tselentis et al. (1996). We performed stabilization

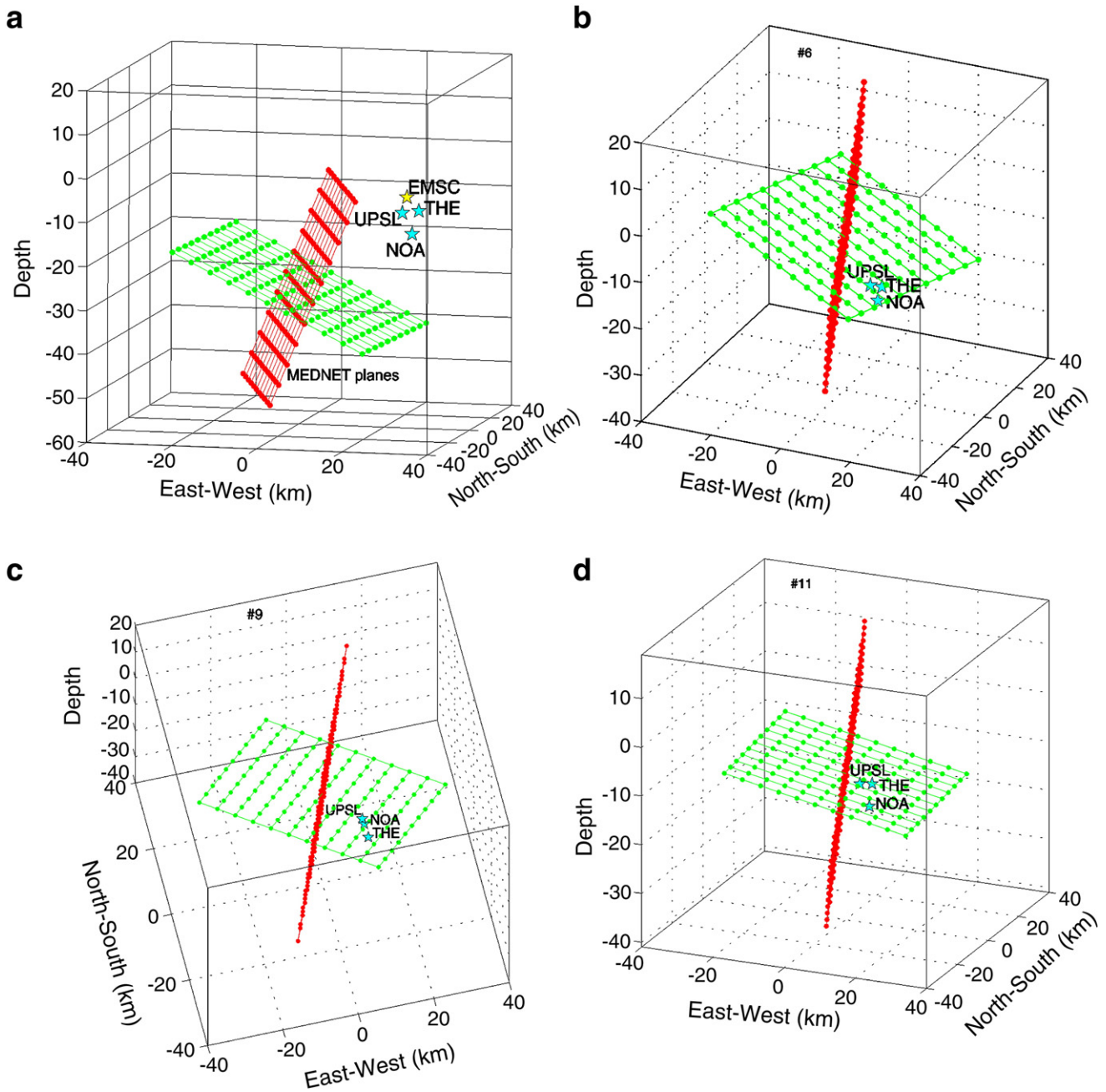


Fig. 6. a) Two nodal planes passing through the centroid (LAT=0 and LON=0), both according to the MT solution of MEDNET, and the hypocenter of EMSC. Event #6. This is an unfavorable case, with hypocenter out of any nodal plane. b, c, and d) Two nodal planes passing through the centroid (LAT=0 and LON=0), both according to the MT solution of this paper, and the hypocenter of this paper. Events #6 (b), #9 (c), and #11 (d). This is the favorable case, with hypocenter in one of the nodal planes, thus indicating the fault plane.

tests for the three major events ($M > 5$) of the sequence and finally we relocated the 33 solutions using HYPODD code (Waldhauser and Ellsworth, 2000). The relocation resulted to a more compact cluster than the initial location. The results show a concentration of the epicenters in the area SSE of the island of Zakynthos. The major events were located at 13 km depth.

In a next step the moment tensors of 24 events of the sequence were calculated by waveform inversion of three-component broadband records of PSLNET. The MT inversion of regional waveforms was performed by the least square method. The centroid was determined by repeated calculations of the MT in a volume grid of trial source positions not far from the hypocenter, aiming at optimizing the fit between the observed and synthetic waveforms.

We combined the hypocenter position derived by HYPO71PC, the DD relocated hypocenters and MT solution (nodal planes) in order to

identify the fault plane responsible for the studied sequence activation. The fault plane is one of the nodal planes passing through the centroid, which contains the hypocenters. The cases of a sub-horizontal nodal plane and a sub-vertical nodal plane were investigated. The case of the sub-vertical plane was rejected since it indicates a back-thrust, which cannot be explained by the tectonic regime of the study area. The case of the sub-horizontal plane was favorable and supported by the hypocenters distribution (Fig. 5b).

The hypocenters of all three major events clearly prefer a sub-horizontal nodal plane, thus indicating just that nodal plane to be the fault plane. Almost all focal mechanisms demonstrate the presence of one low-dip horizontal nodal plane. Since there is limited depth accuracy the definition of a single sub-horizontal plane, along which the hypocenters are distributed comprises uncertainty. Therefore, the final interpretation is that the sub-horizontal plane, dominated the sequence, at the

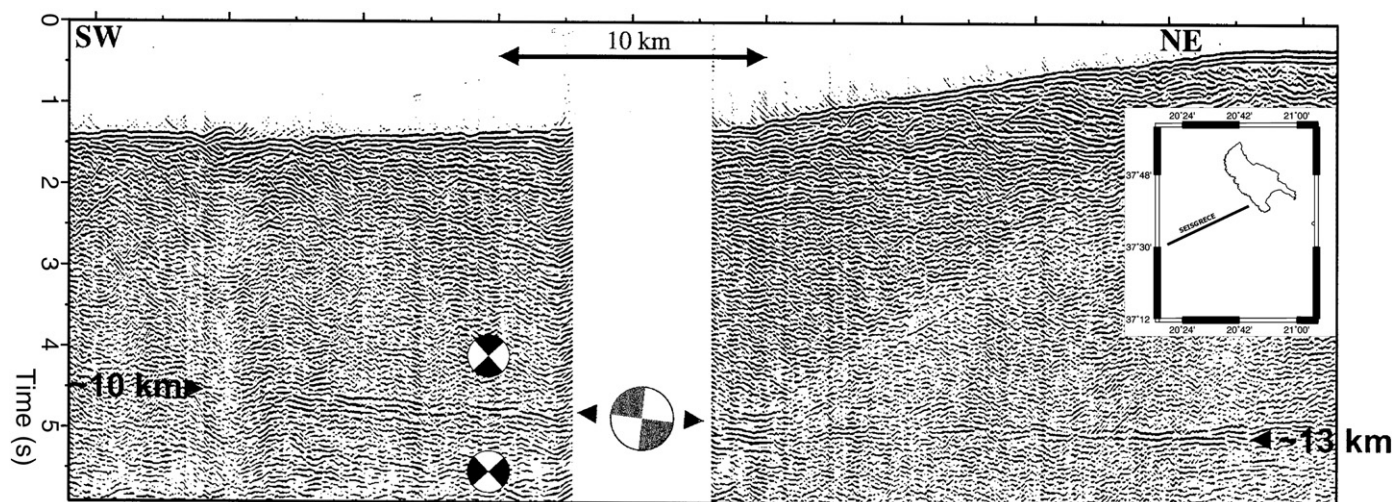


Fig. 7. Multichannel reflection seismic section (line SEISGRECE) revealing a strong reflector interpreted as being the interplate boundary (after Laigle et al., 2004). The big symbol of flat thrust focal mechanism located right at the interplate reflector is representative of the subduction major earthquake as discussed in Clement et al. (2000). The two smaller symbols of focal mechanisms are representative of the mechanisms of local micro-earthquakes from Sachpazi et al. (2000).

approximate depth of about 13 km. In this sense our results support the hypothesis that the interplate boundary of the Hellenic subduction zone plays a role of active surface.

Acknowledgements

The authors would like to thank the Geodynamic Institute of National Observatory of Athens (GEIN, NOA) and the Institute of Engineering Seismology and Earthquake Engineering (ITSAK), for providing readings of the 2006 earthquakes. This work was financially supported by the EC project 004043(GOCE)-3HAZ-CORINTH and the following projects of the Czech Republic: GAUK 279/2006/B-GEO/MFF, GACR 205/07/0502, and MSM 0021620860.

References

- Adamova, P., Sokos, E., Zahradnik, J., 2007. Non-double-couple mechanism and complexity of the Amfilochia Mw-5, Dec. 31, 2002 earthquake. *J. Seismol.* 13, 1–12.
- Anderson, H., Jackson, J., 1987. Active tectonics of the Adriatic region. *Geophys. J. R. Astron. Soc.* 91, 937–983.
- Benetatos, C., Kiratzi, A., Roumelioti, Z., Stavrakakis, G., Drakatos, G., Latoussakis, I., 2005. The 14 August 2003 Lefkada Island (Greece) earthquake: focal mechanisms of the mainshock and of the aftershock sequence. *J. Seismol.* 9, 171–190.
- Brooks, M., Ferentinos, G., 1984. Tectonics and sedimentation in the Gulf of Corinth and the Zakynthos and Kefallinia channels, Western Greece. *Tectonophysics* 101 (1–2), 25–54.
- Chouliaras, G., 2009. Seismicity anomalies prior to 8 June 2008, Mw = 6.4 earthquake in Western Greece. *Nat. Hazards Earth Syst. Sci.* 9 (2), 327–335.
- Clement, C., Hirn, A., Charvis, P., Sachpazi, M., Marnelis, F., 2000. Seismic structure and the active Hellenic subduction in the Ionian islands. *Tectonophysics* 329, 141–156.
- Cushing, E.M., 1985. Evolution structurale de la marge nord ouest Hellenique dans l'île de Levkas et ses environs (Grece nordoccidentale), unpub. Thesis, Université de Paris-Sud, Centred'orsay, Paris 295 pp.
- <http://seismo.geology.upatras.gr/isola/> http://geo.mff.cuni.cz/~jz/tmp/isola06a_release. <http://seis30.karlov.mff.cuni.cz/>.
- Haslinger, F., Kissling, E., Ansorge, J., Hatzfeld, D., Papadimitriou, E., Karakostas, V., Makropoulos, K., Kahle, H.-G., Peter, Y., 1999. 3D crustal structure from local earthquake tomography around the Gulf of Arta (Ionian region, NW Greece). *Tectonophysics* 304, 201–218.
- Hirn, A., Sachpazi, M., Siliqi, R., McBride, J., Marnelis, F., Cernobori, L., the STREAMERS-PROFILES Group, 1996. A traverse of the Ionian Islands front with coincident normal incidence and wide-angle seismics. *Tectonophysics* 264, 35–49.
- Kikuchi, M., Kanamori, H., 1991. Inversion of complex body waves — III. *Bull. Seismol. Soc. Am.* 81, 2335–2350.
- Kiratzi, A.A., Langston, C.A., 1991. Moment tensor inversion, of the 1983 January 17 Kefallinia event of Ionian islands. *Geophys. J. Int.* 105, 529–535.
- Kiratzi, A., Louvari, E., 2003. Focal mechanisms of shallow earthquakes in the Aegean Sea and the surrounding lands determined by waveform modeling: a new database. *J. Geodyn.* 36, 251–274.

- Kiratzi, A., Sokos, E., Ganas, A., Tselentis, A., Benetatos, C., Roumelioti, Z., Serpetsidaki, A., Andriopoulos, G., Galanis, O., Petrou, P., 2008. The April 2007 earthquake swarm near Lake Trichonis and implications for active tectonics in western Greece. *Tectonophysics* 452 (1–4), 51–65 2 June.
- Laigle, M., Sachpazi, M., Hirn, A., 2004. Variation of seismic coupling with slab detachment and upper plate structure along the western Hellenic subduction zone. *Tectonophysics* 391, 85–95.
- McKenzie, D.P., 1972. Active tectonics of the Mediterranean region. *Geophys. J. R. Astron. Soc.* 30, 109–185.
- Meco, S., Aliaj, S., 2000. Geology of Albania Beitrage zur regionalen Geologie der Erde. Gebrueder Borntraeger, Berlin, p. 246.
- Mercier, J., Bousquet, B., Delibasis, N., Drakopoulos, I., Kéraudren, B., Lemeille, F., Sorel, D., 1972. Deformations en compression dans le Quarternaire des rivages ioniens (Cephalonie, Grece) Donnees neotectoniques et seismiques. *Comptes Rendus Acad. Sci. Paris* 275, 2307–2310.
- Mercier, J.L., Carey, E., Philip, H., Sorel, D., 1976. La neotectonique plio-quaternaire de l'Arc Egeen externe et de la mer Egee et ses relations avec la seismicité. *Bull. Soc. Geol. Fr.* 2, 145–151.
- Papadimitriou, E., 1993. Focal mechanism along the convex side of the Hellenic arc: *Bollettino de Geofisica Teorica ed Applicata*, vol. XXXV, pp. 401–426.
- Roumelioti, Z., Ganas, A., Sokos, E., Petrou, P., Serpetsidaki, A., Drakatos, G., 2007. Toward a joint catalogue of recent seismicity in western Greece: preliminary results. *Proc. 11th Int. Congress Geol. Soc. Greece, May 2007, Athens (Greece): Bull. Geol. Soc. Greece*, vol. V XXXX, pp. 1257–1267.
- Sachpazi, M., Hirn, A., Clement, C., Haslinger, F., Laigle, M., Kissling, E., Charvis, P., Hello, Y., Lepine, J.-C., Sapin, M., Ansorge, J., 2000. Western Hellenic subduction and Cephalonia transform: local earthquakes and plate transport and strain. *Tectonophysics* 319, 301–319.
- Sokos, E., Zahradnik, J., 2008. ISOLA — A Fortran code and a Matlab GUI to perform multiple-point source inversion of seismic data. *Comput. Geotech.* 34, 967–977.
- Somerville, P., Irikura, K., Graves, R., Sawada, S., Wald, D., Abrahamson, N., Iwasaki, Y., Kagawa, T., Smith, N., Kowada, A., 1999. Characterizing crustal earthquake slip models for the prediction of strong ground motion. *Seismol. Res. Lett.* 70, 59–80.
- Sorel, D., Lemeille, F., Limond, J., Nesteroff, W.D., Sebrier, M., 1976. Mise en evidence de structures compressives sous-marines plio-pleistocenes dans l'arc egeen externe au large de Levkas (Iles Ioniennes, Grace). *C.R. Acad. Sci. Paris D (282)*, 2045–2048.
- Stiros, S.C., Pirazzoli, P.A., Laborel, J., Laborel-Deguen, F., 1994. The 1953 earthquake in Cephalonia (western Hellenic Arc): coastal uplift and halotectonic faulting. *Geophys. J. Int.* 117 (3), 834–849.
- Tselentis, G.-A., Melis, N.S., Sokos, E., Papatsimpa, K., 1996. The Egean June 15, 1995 (6.2 ML) earthquake, Western Greece. *Pure Appl. Geophys.* 147, 83–98.
- Tselentis, G.-A., Sokos, E., Martakis, N., Serpetsidaki, A., 2006a. Seismicity and seismotectonics in Epirus, Western Greece: results from a microearthquake survey. *Bull. Seismol. Soc. Am.* 96 (5), 1706–1717.
- Tselentis, G.-A., Sokos, E., Serpetsidaki, A., Zahradnik, J., Jansky, J., Plicka, V., 2006b. New satellite BB network of western Greece and its application to the M5 earthquake sequence of Zakynthos, April 2006. *Abstract Book First European Conference on Earthquake Engineering and Seismology, Geneva, Switzerland*, p. 273.
- Underhill, J.R., 1988. Triassic evaporites and Plio-Quaternary diapirism in western Greece. *J. Geol. Soc. Lond.* 145, 269–282.
- Underhill, J.R., 1989. Late Cenozoic deformation of the Hellenide foreland, western Greece. *Geol. Soc. Am. Bull.* 101, 613–634.

- Van Hinsbergen, D.J.V., der Meer, J.Z.D.G., Zachariasse, W.J., Meulen Kamp, Z.J.E., 2006. Deformation of western Greece during Neogene clockwise rotation and collision with Apulia. *Int. J. Earth Sci. Geol. Rundsch.* 95, 463–490.
- Waldhauser, F., 2001. HypoDD - A program to compute double-difference hypocenter locations, U.S. Geological Survey open-file report, 113pp.
- Waldhauser, F., Ellsworth, W.L., 2000. A double-difference earthquake location algorithm: method and application to the Northern Hayward fault California. *Bull. Seismol. Soc. Am.* 90, 1353–1368.
- Zahradnik, J., Serpetsidaki, A., Sokos, E., Tselentis, G.-A., 2005. Iterative deconvolution of regional waveforms and double-event interpretation of the 2003 Lefkada earthquake Greece. *Bull. Seismol. Soc. Am.* 95, 159–172.
- Zahradnik, J., Sokos, E., Tselentis, G.-A., Martakis, N., 2008. Non-double-couple mechanism of moderate earthquakes near Zakynthos, Greece, April 2006; explanation in terms of complexity. *Geophys. Prospect.* 56 (3), 341–356.